Journal of Experimental Botany, Vol. 70, No. 19 pp. 5189–5203, 2019
doi:10.1093/jxb/erz276 Advance Access Publication June 6, 2019
This paper is available online free of all access charges (see https://academic.oup.com/jxb/pages/openaccess for further details)

RESEARCH PAPER

The HD-Zip transcription factor LcHB2 regulates litchi fruit abscission through the activation of two cellulase genes

Caiqin Li[1,2,3,†], Minglei Zhao[1,2,†], Xingshuai Ma[1,2,†], Zhenxi Wen[1,2], Peiyuan Ying[1,2], Manjun Peng[1,2], Xiping Ning[1], Rui Xia[1,2], Hong Wu[1,*] and Jianguo Li[1,2,*]

[1] State Key Laboratory for Conservation and Utilization of Subtropical Agro-Bioresources, South China Agricultural University, Guangzhou, 510642, China
[2] Guangdong Litchi Engineering Research Center, College of Horticulture, South China Agricultural University, Guangzhou, 510642, China
[3] Guangdong Provincial Key Laboratory of Postharvest Science of Fruits and Vegetables, College of Horticulture, South China Agricultural University, Guangzhou, 510642, China

[†] These authors contributed equally to this work.
* Correspondence: jianli@scau.edu.cn or wh@scau.edu.cn

Received 15 December 2018; Editorial decision 28 May 2019; Accepted 30 May 2019

Editor: Ariel Vicente, CONICET- National University of La Plata, Argentina

Abstract

Cellulases play important roles in the shedding of plant organs; however, little is yet known about the functions of cellulase genes during the process of organ abscission. Abnormal fruitlet abscission is a serious problem in the production of litchi (*Litchi chinensis*), an economically important fruit widely grown in South Asia. In this study, two abscission-accelerating treatments (carbohydrate stress and application of ethephon) were evaluated in litchi fruitlets. Cell wall degradation and cell separation were clearly observed in the abscission zones of treated fruitlets, consistent with enhanced cellulase activities and reduced cellulose contents. The expression of two cellulase genes (*LcCEL2* and *LcCEL8*) was strongly associated with abscission. Floral organs of transgenic Arabidopsis overexpressing *LcCEL2* or *LcCEL8* showed remarkably precocious abscission. Electrophoretic mobility shift assays and transient expression experiments demonstrated that a novel homeodomain-leucine zipper transcription factor, LcHB2, could directly bind to and activate HD-binding *cis*-elements in the *LcCEL2* and *LcCEL8* promoters. Our results provide new information regarding the transcriptional regulation of the cellulase genes responsible for cell wall degradation and cell separation during plant organ shedding, and raise the possibility of future manipulation of litchi fruitlet abscission by modulation of the activities of these two cellulases.

Keywords: Cell separation, cellulase, fruit abscission, HD-Zip, *Litchi chinensis*, lychee.

Introduction

Litchi (*Litchi chinensis*) is an important tropical fruit crop that is currently cultivated in over 20 countries. Under normal conditions, litchi produces many inflorescences with 100–250 female flowers per inflorescence. However, more than 95%

Abbreviations: AP, apical portion; AZ, abscission zone; BAC, BEAN ABSCISSION CELLULASE; BCECF, 2′,7′-Bis(2-carboxyethyl)-5-(and-6)-carboxyfluorescein; BP, basal portion; bZIP, basic leucine zipper; CBD, cellulose-binding domain; CBM, carbohydrate-binding module; CEL, cellulase; ETH, ethephon; FAZ, fruit abscission zone; GFP, green fluorescent protein; GPD, girdling plus defoliation; GUS, β-glucuronidase; HD, homeodomain; HD-Zip, homeodomain-leucine zipper; LZ, leucine-zipper; PAS, periodic acid-Schiff stain; pI, isoelectric point; qRT-PCR, quantitative real-time PCR; TF, transcription factor.

of the initial female flowers do not develop into mature fruit (Stern *et al.*, 1995; Mitra *et al.*, 2003). For normal-seeded litchi cultivars, three distinct waves of fruit abscission are observed (Yuan and Huang, 1988). The first occurs around the end of week 1 after full bloom with ~60% of fruitlet loss. The second wave occurs around the end of week 3 after full bloom, with about half of the remaining fruitlets being abscised. Soon after that, a small third wave begins. For aborted-seed cultivars, an additional pre-harvest abscission occurs 2–3 weeks before harvest and only ~60% of the remaining fruit survive (Yuan and Huang, 1988). In the period 2013–2015, the average yield of litchi in China was only 3.8 t ha^{-1} (Qi *et al.*, 2016). The excessive abscission of flowers/fruitlets is one of the main factors responsible for the universally low productivity in litchi (Yuan and Huang, 1988; Mitra *et al.*, 2003).

An essential event during abscission is the separation of specialized cells within the abscission zone (AZ), which is located at the base of the organ that will be shed (Patterson, 2001; Estornell *et al.*, 2013). The breakdown of cell wall components in AZ cells is dependent upon the activities of cell wall-specific hydrolases (Roberts *et al.*, 2002). Endo-(1,4)-β-D-glucanases (or cellulases, CELs) are responsible for cellulose degradation and are thought to be important for organ abscission (Sexton and Roberts, 1982). In bean (*Phaseolus vulgaris*), the structural integrity of the petiole AZ is lost during abscission owing to cellulase activity (Horton and Osborne, 1967), which is the result of *de novo* synthesis of a high-salt extractable cellulase named BEAN ABSCISSION CELLULASE (BAC) (Reid and Lewis, 1974; Tucker *et al.*, 1991). In tomato (*Solanum lycopersicum*), three cellulase genes (*SlCel1*, *SlCel2*, and *SlCel5*) are found to be highly expressed in the pedicel AZs where cell separation occurs (Lashbrook *et al.*, 1994; del Campillo and Bennett, 1996). Antisense suppression of *SlCel1* mRNA accumulation reduces flower abscission by up to one third (Lashbrook *et al.*, 1998), while knocking down the expression of *SlCel2* results in greater force being required to remove fruits (Brummell *et al.*, 1999). *SlCel5* has been used as a cell wall-degradation marker gene for microarray analysis during ethylene-promoted tomato flower abscission (Wang *et al.*, 2013). In Arabidopsis, there are 25 putative cellulase family members (Urbanowicz *et al.*, 2007). A transcriptomic analysis using laser-capture microdissection has reported the induction of cellulase family members *AtCel3* (At1g71380), *AtCel5* (At1g22880), *EGase10* (At1g75680), and *EGase11* (At2g32990) in stamen AZs and their involvement in cell separation (Lashbrook and Cai, 2008). Recently, a newly discovered cellulase gene, *AtCEL6* (At4g39010), has been shown to promote silique dehiscence by promoting cell disintegration in the separation layer (He *et al.*, 2018). Overall, these results suggest that enhancement of the expression and activity of cellulases is important for cell separation during organ abscission.

To date, at least 10 different abscission-associated cellulase genes have been found in fruit crops, including *ppEG1* and *ppEG4* in peach (*Prunus persica*) (Trainotti *et al.*, 1997, 2006), *PaCel1* in avocado (*Persea americana*) (Tonutti *et al.*, 1995), *MdEG1* in apple (*Malus×domestica*) (Li and Yuan, 2008), and *CitCEL3*, *CitCEL6* (*CsCEL-a1*), *CitCEL10*, *CitCEL22*, and *CsCEL-b1* in citrus (*Citrus sinensis*) (Kazokas and Burns, 1998; Merelo *et al.*, 2017). However, the functions of these cellulases during abscission as well as their underlying mechanisms are still largely unknown.

Promoter analysis of *BAC* gene during bean leaf abscission has shown that ethylene positively induces its expression, whereas auxin strongly suppresses expression (Koehler *et al.*, 1996). However, because the core elements for ethylene and auxin responses have not been found in the *BAC* promoter (Koehler *et al.*, 1996), these hormones probably affect *BAC* expression indirectly. Further analysis by Tucker *et al.* (2002) implicated three TGA-type basic leucine zipper (bZIP) transcription factors (TFs) in activating the *BAC* promoter. The Arabidopsis HD-Zip (homeodomain-leucine zipper) HDG11 can directly up-regulate the cellulase gene At2g32990 during the elongation of roots (Xu *et al.*, 2014). Members of the HD-Zip gene family in higher plants encode TFs containing a DNA-binding homeodomain (HD) and an adjacent leucine-zipper domain (bZIP, also known as an LZ domain) (Ariel *et al.*, 2007). The HD-Zip family comprises four subfamilies (HD-Zip I–IV), each of which plays specific roles in plant development (Ariel *et al.*, 2007); however, whether they are involved in the shedding of plant organs has yet not been studied.

Carbohydrate deficiency and hormone effects are the two main factors considered to affect fruit drop in litchi (Yuan and Huang, 1988; Hieke *et al.*, 2002). Comprehensive transcriptome profiling studies under carbohydrate stress and ethylene-induced abscission have been documented in our previous studies (Li et al., 2015a, 2015b) that identified many genes potentially involved in litchi fruitlet abscission. These studies revealed several genes with putative functions related to cell wall modification, as well as TFs such as *HD-Zip* genes. However, which genes are essential for abscission and how they are regulated is not yet known. In the present study, two cellulase genes (*LcCEL2* and *LcCEL8*) and a novel HD-Zip TF (*LcHB2*) were identified as key genes associated with fruitlet abscission in litchi. Ectopic expression of *LcCEL2* and *LcCEL8* in Arabidopsis showed that these genes could induce precocious floral organ abscission. Further, LcHB2 was shown to directly bind the promoters and activate expression of *LcCEL2* and *LcCEL8*. These results add to our understanding of the transcriptional regulatory mechanisms by which cellulase genes are involved in plant organ shedding.

Materials and methods

Plant materials and treatments

Several 12-year-old litchi trees (*Litchi chinensis* Sonn. cvs. 'Zhumuru' and 'Kulin') were randomly chosen in an orchard at the South China Agricultural University (Guangzhou, China) in 2015. Thirty fruitlet-bearing shoots of similar diameter (about 5–8 mm) growing in different directions were tagged on each tree. At 30 d after anthesis, half of the fruitlet-bearing shoots of 'Zhumuru' were treated by girdling (removing a 0.5-cm wide ring of bark and cambium from around the base of the branch) and by defoliation beyond the ring of girdling, hereafter referred to as the GPD treatment ('girdling plus defoliation'; Supplementary Fig. S1A at *JXB* online). The remaining untreated shoots were used as the control. Half of the fruitlet-bearing shoots of 'Kulin' were dipped in a solution containing 250 mg l^{-1} ethephon and 0.05% Tween® 80 surfactant for 1 min (designated as the ETH treatment) and the remaining shoots

were dipped in water and used as the control. Of the 15 treated shoots, three were used for monitoring the fruitlet abscission dynamics and the remainder were used for tissue sampling. We calculated the cumulative rate of fruitlet abscission according to our previous study (Kuang *et al.*, 2012). Using a sharp razor blade, different regions of the fruitlet pedicels were sampled based around the fruitlet abscission zone (FAZ), which appears as a visible sunken ring of ~2 mm in length (Supplementary Fig. S1B). In addition to the FAZ, a region of the pedicel of ~2 mm in length between the FAZ and the fruitlet-bearing stem was cut and designated as the basal portion (BP). A region of similar length between the FAZ and the fruitlet was also excised and designated as the apical portion (AP). After separation, the FAZ, BP, and AP tissues were quickly frozen in liquid nitrogen and stored at –80 °C. Each tree was considered a biological replicate and three replicates were performed for each treatment.

Microscopic and histochemical observations

Samples of the FAZs (1 mm length) were fixed in 4% paraformaldehyde with 1% glutaraldehyde at 4 °C for 24 h. Samples were then dehydrated in an ethanol series and embedded in paraffin prior to cutting 10-μm sections. Sections were stained for morphological observation using 1% (w/v) Safranin O (Amresco, Solon, USA) and 1% (w/v) Fast Green FCF (Merck, Overijse, Belgium) (Zou *et al.*, 2011). Insoluble polysaccharides were visualized by periodic acid–Schiff (PAS) staining (Feder and O'Brien, 1968), and cellulose was stained using 0.01% Calcofluor White (Sigma-Aldrich) and the carbohydrate-binding module CBM3a (PlantProbes, Leeds, UK).

Measurement of cellulase activity and cellulose content

Cellulose contents were determined using the anthrone method (Viles and Silverman, 1949). Cellulase activities were measured using a tissue-blotting and gel-diffusion method (Bourgault and Bewley, 2002; Yang *et al.*, 2015) for litchi FAZs and by the DNS (3,5-dinitrosalicylic acid) method for Arabidopsis leaves (Wang *et al.*, 1998), respectively.

Sequence analysis and quantitative real-time PCR (qRT-PCR)

Protein sequences of all candidate genes were retrieved from the litchi genome database (http://litchidb.genomics.cn/page/species/index.jsp), the Arabidopsis genome database (https://www.arabidopsis.org/index.jsp), and the plant genomics resource (Phytozome version 12.1; https://phytozome.jgi.doe.gov/pz/portal.html). Multiple alignments were performed using the ClustalW 1.83 (Thompson *et al.*, 1994) and GeneDoc software (Nicholas, 1997). Phylogenetic trees were constructed using neighbor-joining analysis in MEGA 7 (Tamura *et al.*, 2011) with the Poisson correction model, pairwise deletion method, and bootstrapping with 1000 replicates. Total RNA was isolated using a Column Plant RNAout 2.0 Kit (Tiandz, Beijing, China). qRT-PCR was performed using GoTaq® qPCR Master Mix (Promega) on a CFX96 Real-Time PCR System (Bio-Rad). Gene expression levels were normalized using *LcEF-1α* and *LcGAPDH* as the internal reference genes for litchi (Zhong *et al.*, 2011) and *AtUBQ* for Arabidopsis (Ying *et al.*, 2016). Three biological replicates were performed. All primers used in this study are listed in Supplementary Table S1.

Subcellular localization analysis

Coding sequences of *LcCEL2* (1863 bp), *LcCEL8* (1491 bp), and *LcHB2* (684 bp), each lacking a stop codon, were subcloned into the pEAQ-HT-GFP vector (Ye *et al.*, 2016) and fused in-frame with the green fluorescent protein (GFP) sequence under the control of the CaMV 35S promoter using a ClonExpress II One Step Cloning Kit (Vazyme, Nanjing, China). *Agrobacterium tumefaciens* strain GV3101 harboring LcCEL2-GFP, LcCEL8-GFP, LcHB2-GFP, or the positive control were individually infiltrated into the abaxial side of leaves of tobacco (*Nicotiana benthamiana*) or inoculated into plasmolytic epidermal cells of onion (*Allium cepa*). GFP fluorescence signals were visualized using an Axioskop 2 Plus fluorescence microscope (Zeiss). All assays were performed with at least three replications.

Generation of transgenic plants and BCECF fluorescence analyses

Coding sequences of *LcCEL2* and *LcCEL8*, each lacking a stop codon, were subcloned under the control of the CaMV 35S promoter into the pCAMBIA1302 vector, and then these constructs were individually transformed into Arabidopsis Columbia-0 (Col-0) ecotype plants using the floral dip method (Clough and Bent, 1998). Further phenotypic analysis and BCECF [2',7'-Bis-(2-carboxyethyl)-5-(and-6)-carboxyfluorescein] fluorescence assays were conducted as described by Ying *et al.* (2016). Flower position numbers were counted from the first flower with visible white petals at the top of the inflorescence.

Histochemical GUS assays

Genomic DNA was extracted from litchi leaves following the CTAB protocol (Puchooa, 2004). The promoter fragments of *LcCEL2* (2215 bp), *LcCEL8* (2192 bp), and *LcHB2* (2048 bp) were subcloned into the pCAMBIA1391 vector upstream of the GUS (β- glucuronidase)-coding region (Supplementary Fig. S2A). These constructs were then individually transformed into Arabidopsis Col-0 plants. Inflorescences, siliques, and cauline leaves were incubated in GUS staining buffer (Waryong, Beijing, China) for 2–4 h at 37 °C in the dark. The samples were then decolorized in 100% ethanol, cleared in transparent solution (30 g Chloral hydrate, 10 ml glycerol, 30 ml water) overnight, and visualized using a Zeiss SV11 stereoscope.

Dual-luciferase reporter assays

Diagrams of the effector and reporter vectors used for dual-luciferase reporter assays are shown in Supplementary Fig. S2B, C. The effector and reporter plasmid constructs were co-transformed into tobacco leaves using *Agrobacterium* infiltration. After 2–3 d, activities of the LUC and REN luciferases were measured using the Dual-Luciferase® Reporter Assay System (Promega) on a Luminoskan Ascent Microplate Luminometer (ThermoFisher Scientific). The results were calculated as the ratio of fluorescence of LUC to that of REN. At least six biological replications were performed for each combination of effector and reporter.

Electrophoretic mobility shift assays (EMSA)

LcHB2 was cloned into the pET-28a(+) vector and expressed in *E. coli* BL21 (DE3) cells. Recombinant proteins were purified and used for EMSAs along with biotin-labeled fragments (~50 bp) of the *LcCEL2* and *LcCEL8* promoters. The same fragment, but unlabeled, was used as a competitor, while a probe within the mutant HD-binding *cis*-elements (interchanging A with G or T with C) was used as a mutant competitor in the assay. EMSAs were performed using a LightShift™ Chemiluminescent EMSA Kit (ThermoFisher Scientific). After cross-linking, the membrane was detected by the chemiluminescence method on a ChemiDoc™ MP Imaging System (Bio-Rad).

Accession numbers

Gene accession numbers are listed in Supplementary Tables S2–S4.

Results

Effects of carbohydrate stress and ethephon treatments on litchi fruitlet abscission

To determine the effect of girdling plus defoliation (GPD), which leads to carbohydrate stress, and application of ethephon

(ETH) on fruitlet abscission, the rate of fruitlet drop under each treatment was recorded each day for 5 d after the treatments. Compared to the control, GPD dramatically accelerated fruitlet drop, with a rate of 77.27% at day 2 and up to 96.84% at day 3 (Fig. 1A). At day 3, a clear white ring (the abscission ring) could be seen to have formed across the FAZ, which was caused by fracturing of the epidermis (Fig. 1B). Although the fruitlets remain attached to the branch, they could easily be detached with only a light external force. Under the ETH treatment, the rate of abscission gradually increased and reached a maximum of 92.1% at day 5, when visible abscission rings were again observed (Supplementary Fig. S3A, B). In contrast, fruitlet drop was much slower in the controls, with a cumulative abscission rate of only 18.99% at day 3 in the control for GPD and of 14.5% at day 5 in the control for the ETH treatment.

Cell disruption and separation initiate in the FAZs during abscission

Microscopic observations revealed clear evidence of cell breakdown in the FAZ during litchi fruitlet abscission. The FAZ usually included 7–10 layers of small, dense, oblong cells (Fig. 1C–E; Supplementary Fig. S3C–E). At 2 d following GPD treatment, cortical cells in the FAZ became enlarged and less Safranin O/Fast Green staining was absorbed. Separation of cells in the epidermis and cortex then occurred at the abscission site (Fig. 1D). Soon afterwards, the FAZ cells expanded further and disintegrated, leading to the formation of an intercellular space. As a result, a fracture appeared in the FAZ and further progressed toward the vascular bundle and pith, indicating that cell separation occurred at the FAZ after GPD treatment (Fig. 1D, E). In the FAZ from ETH-treated branches, enlarged and distorted cells appeared on day 3, and the separation layer was visible on day 5 (Supplementary Fig. S3D, E). In contrast, the FAZ of the controls showed no cell expansion and separation at day 3 after GPD and day 5 after ETH (Fig. 1C, E; Supplementary Fig. S3C, E). Both treatments significantly decreased the number of FAZ cells (only 29% of the control at day 3 after GPD and 49% of the control at day 5 after ETH treatment), and the cells were longer and wider than those in the controls (Fig. 1F; Supplementary Fig. S3F). All the results indicated that the enlargement of FAZ cells was involved in the processes of cell disruption and separation during fruitlet abscission.

Cellulose degradation occurs upon disruption of FAZ cells during abscission

PAS staining was used to characterize the anatomical locations of insoluble polysaccharides in the FAZs after the GPD and ETH treatments. The walls of the separation layer cells in the FAZs showed a decreased affinity for PAS compared to those of the controls, indicating lower contents of insoluble cell wall polysaccharides in the FAZ cells (Fig. 2A). Calcofluor White staining and CBM3a labeling were further used to investigate the changes in cellulose contents. In control the FAZs, Calcofluor White staining of the walls of cells in the separation layer remained high (Fig. 2B), and no clear differences in CBM3a labeling were detected throughout the experiment (Fig. 2C). In contrast, at later stages following the GPD and ETH treatments, remarkably low intensities of Calcofluor White and CBM3a labeling signals were observed in FAZ cells, specifically where cell separation occurred (Fig. 2B, C).

Cellulose concentrations in the FAZs at day 3 after the GPD treatment and at day 5 after the ETH treatment were much less than those of the controls (Fig. 3A, B). Further, the concentration of cellulose was significantly negatively correlated with fruitlet abscission rates (r=−0.51) (Fig. 3C). Compared with the control, cellulase activities in the FAZs were significantly higher at day 2 after the GPD treatment and at day 4 after the ETH treatment, and reached their highest levels at day 3 (~7.2-fold) after GPD and at day 5 (~3.2-fold) after ETH treatment (Fig. 3D, E). Cellulase activities were significantly and positively correlated with fruitlet abscission rates (r=0.849) (Fig. 3F). In contrast, control FAZs exhibited extremely low or non-detectable cellulase activity. Collectively, these results indicated that the increase in cellulase activity in the FAZ cells caused loss of cellulose content in cell walls, and directly resulted in the enhancement of fruitlet abscission.

Two cellulase genes are associated with fruitlet abscission

A total of 20 cellulase genes, designated as *LcCEL1*–*LcCEL20*, were identified in the litchi genome (Supplementary Table S2). The expression of three putative target genes (*LcCEL2*, *LcCEL8*, and *LcCEL9*) was found to be significantly higher during fruitlet abscission according to our previous RNA-Seq transcriptome analysis (Supplementary Fig. S4, Supplementary Table S5; Li *et al.*, 2015b). To further confirm the expression of these genes, we performed qRT-PCR analysis and found that the expression of *LcCEL2* and *LcCEL8* was induced in FAZ tissues during the abscission process. Compared with the control, the expression of *LcCEL2* in FAZs after GPD treatment significantly increased from day 2 and reached its highest level at day 3 (~3.5-fold) (Fig. 3G). Expression of *LcCEL8* in FAZs increased more dramatically, by ~70-fold at day 2 and ~40-fold at day 3 after the GPD treatment (Fig. 3J). During ETH-induced abscission, both *LcCEL8* and *LcCEL2* expression in FAZs strongly increased from day 4 onward and reached their highest levels (~23-fold and ~4.7-fold, respectively) at day 5 (Fig. 3H, K). Thus, *LcCEL2* and *LcCEL8* expression in FAZs was significantly correlated with fruitlet abscission rates (r=0.924 and 0.813, respectively) (Fig. 3I, L). Moreover, when the expressions of *LcCEL8* and *LcCEL2* were examined in the two pedicel regions flanking the FAZs, the apical portion (AP) at the fruitlet side and the basal portion (BP) at the proximal pedicel side (Supplementary Fig. S1B), *LcCEL2* and *LcCEL8* transcripts accumulated exclusively in the FAZ under both GPD and ETH treatments (Fig. 3G, H, J, K). Although transcriptomic data from abscising fruitlets showed higher RPKM values for *LcCEL9* under GPD and ETH treatments than in the control group (Supplementary Fig. S4, Supplementary Table S5), the accumulation of *LcCEL9* transcripts could not be detected by qRT-PCR. We therefore

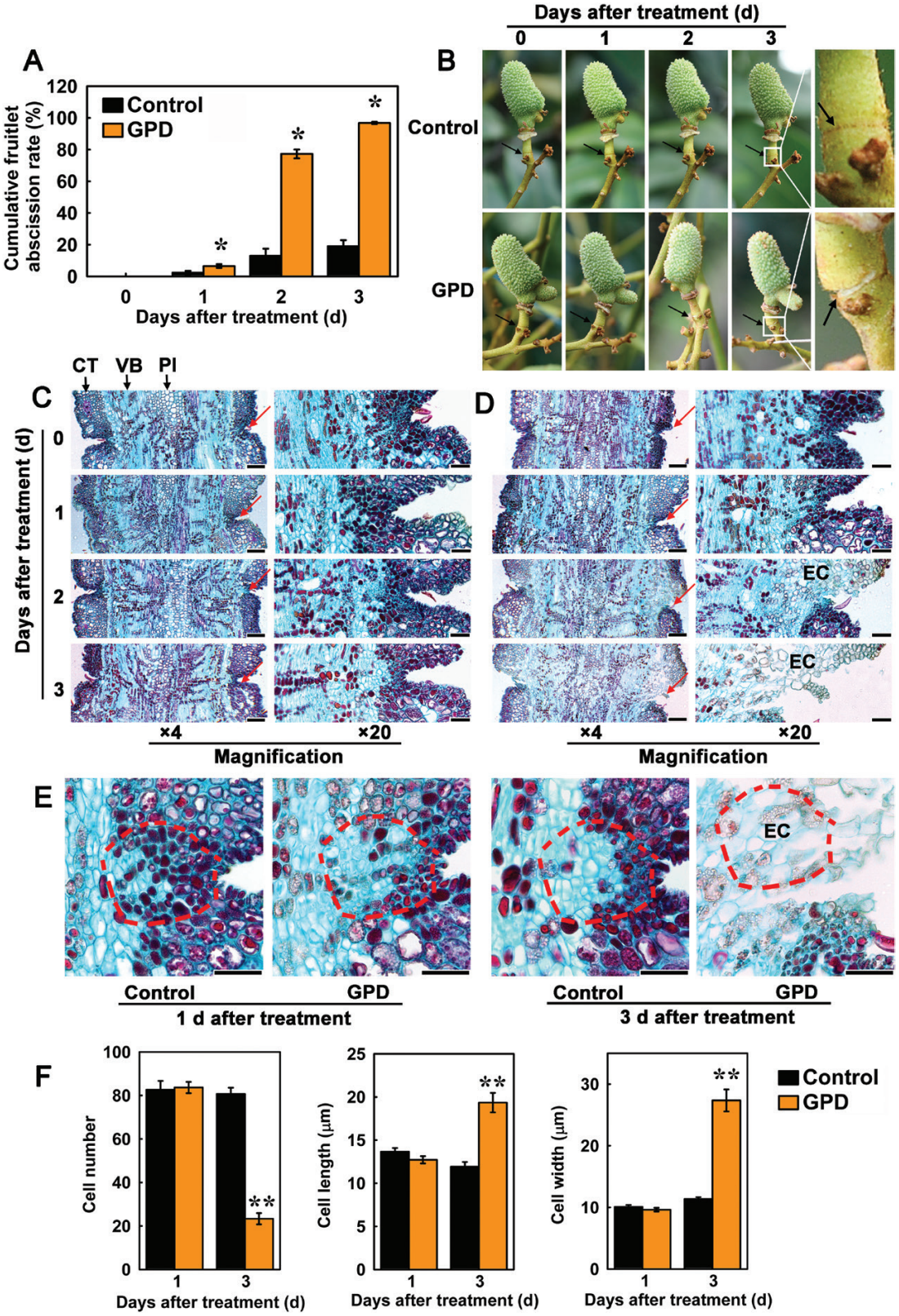

Fig. 1. Effects of carbohydrate stress treatment (girdling plus defoliation, GPD) on the cumulative fruitlet abscission rate, phenotypic performance, and cell separation in the fruitlet abscission zone (FAZ) of litchi. (A) Cumulative fruitlet abscission rate. Data are means (±SE) from three replicates. Significant differences between GPD and control branches were determined using Student's *t*-test: **P*<0.05. (B) Phenotypic characteristics of FAZs during the fruitlet abscission process. The images on the right show magnifications of the FAZs at 3 d after GPD treatment. Arrows indicate the location of the abscission layers. (C, D) Longitudinal sections of the FAZs from fruitlets from control (C) and GPD-treated (D) branches stained with Safranin O and Fast Green at 4× and 20× magnification, respectively. Arrows indicate the location of the abscission layers. CT, cortex; EC, expanding cells; PI, pith; VB, vascular bundle. Scale bars are 200 μm at 4× magnification and 50 μm at 20× magnification. (E) Longitudinal sections of FAZs from control and GPD-treated branches at 1 d and 3 d after treatment. Scale bars are 50 μm. (F) Cell number, cell length, and cell width of the FAZs. A vision field of ~10 000 μm^2 (shown by the dashed lines in E) were used to count cell numbers. Up to 90 cells were used to measure the length and width. Significant differences between GPD and control branches were determined using Student's *t*-test: ***P*<0.01, for at least three longitudinal sections.

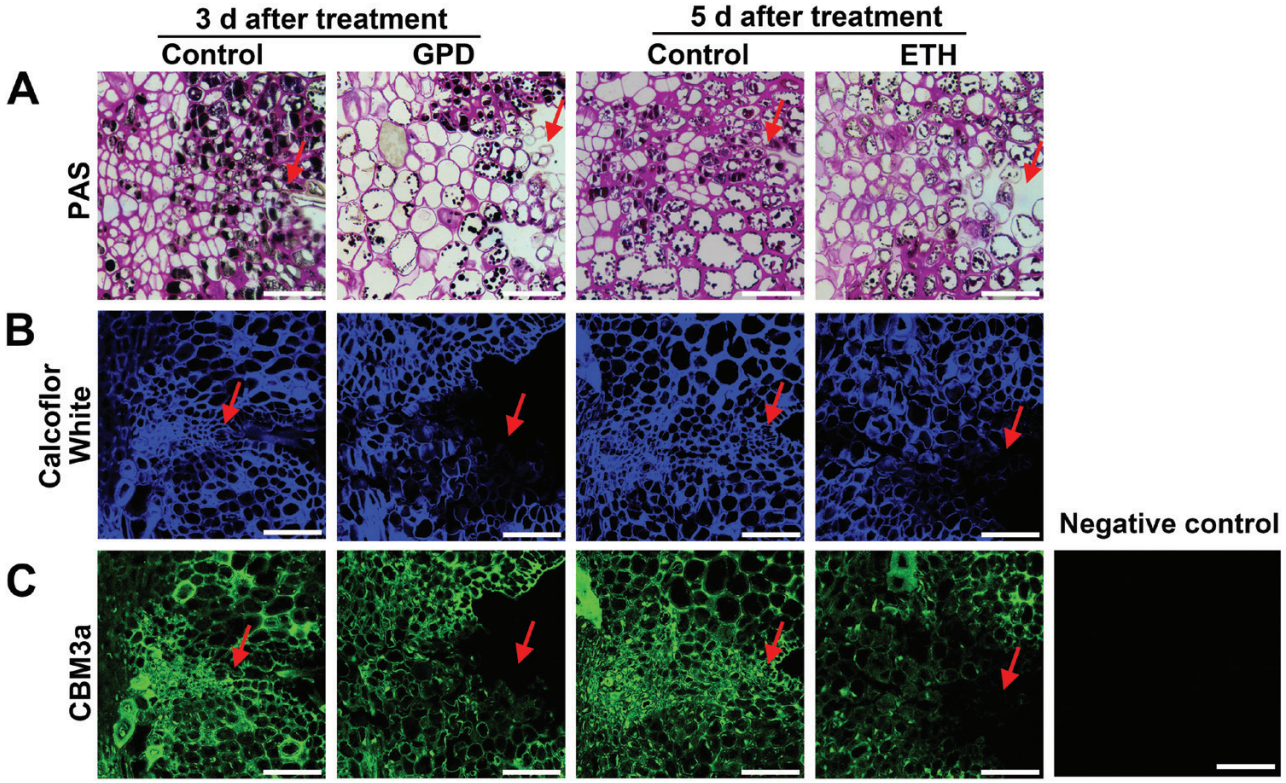

Fig. 2. Localization of polysaccharides and cellulose epitopes in fruitlet abscission zone (FAZ) cells during abscission in litchi. (A) Periodic acid–Schiff reactive (PAS) staining for insoluble carbohydrates in longitudinal sections of the FAZs. (B) Calcofluor White staining for cellulose in longitudinal sections of the FAZs. Calcofluor White is a special fluorescent stain that binds strongly to cellulose (Hughes and McCully, 1975). (C) Staining with antibody CBM3a in longitudinal sections of the FAZs. CBM3a is a CBM (carbohydrate-binding module) probe for crystalline cellulose (Blake *et al.*, 2006). The micrographs show the FAZs from fruitlets of control branches and branches at 3 d after girdling plus defoliation (GPD) or 5 d after treatment with ethephon (ETH). Arrows indicate the location of the abscission layer. Scale bars are 50 μm.

chose *LcCEL2* and *LcCEL8* for further analysis as these two genes could be strongly associated with fruitlet abscission.

Ectopic expression of LcCEL2 *and* LcCEL8 *activate abscission of floral organs in Arabidopsis*

To further investigate the functions of *LcCEL2* and *LcCEL8*, the *in vivo* subcellular localizations of the LcCEL2 (621 aa) and LcCEL8 (497 aa) proteins were examined. We found that LcCEL2-GFP and LcCEL8-GFP were exclusively localized to cell walls when transiently expressed in tobacco leaves and plasmolytic onion epidermal cells (Fig. 4A). This suggested that LcCEL2 and LcCEL8 are cell wall-localized proteins, which agrees with their potential functions in cell wall degradation. We then transgenically expressed *LcCEL2* and *LcCEL8* under the control of the CaMV 35S promoter in Arabidopsis. Homozygous *35S::LcCEL2* and *35S::LcCEL8* transgenic lines were obtained for further experiments. Both cellulase activities and expression of *LcCEL2* and *LcCEL8* in the transgenic lines were significantly higher than those of the corresponding wild-type (Col-0) (Fig. 4B, C). The phenotypes of the flowers or siliques at specific flower positions on Col-0, *35S::LcCEL8*, and *35S::LcCEL2* transgenic plants were examined. Both *35S::LcCEL2* and *35S::LcCEL8* plants dropped their flowers first at position 5 or 6 (Fig. 4D; Supplementary Fig. 5A, B). In contrast, Col-0 plants first abscised their flowers at position 8 (Fig. 4D). This suggested that transgenic expression of *LcCEL2* and *LcCEL8* in Arabidopsis could induce precocious abscission of floral organs.

Sundaresan *et al.* (2014) demonstrated that cytosolic pH increases in AZ cells concomitant with organ abscission. We also observed an early increase in the cytosolic pH of AZ cells of the floral organs using the pH-sensitive indicator BCECF. Green fluorescence from BCECF was normally observed in the AZ of flowers beginning at position 5 in the wild-type plants (Fig. 4E). In contrast, the lines expressing *35S::LcCEL2* and *35S::LcCEL8* showed much earlier fluorescence signals that could be detected first in flowers at position 3 (Fig. 4E; Supplementary Fig. 5C), consistent with the precocious abscission phenotypes of these transgenic lines.

Next, the 5′ sequences upstream of the transcription start sites of *LcCEL2* and *LcCEL8* genes were amplified from the genome of litchi. The sizes of fragments amplified from these genomic regions were 2215 bp and 2192 bp for *LcCEL2* and *LcCEL8*, respectively (Supplementary Dataset S1). We then transgenically expressed a GUS reporter gene fused downstream of the native *LcCEL2* and *LcCEL8* promoters to assess the strength and specificity of their expression in Arabidopsis. Both *LcCEL2* and *LcCEL8* were successfully expressed in Arabidopsis floral AZs during organ abscission (Fig. 5). GUS signals in *proCEL2::GUS* plants were strongly detected in AZs of flowers from position 5 to 9, and were also apparent in stigma tissues, anther filaments, and petals, and in the dehiscence and seed-shedding zones of the siliques (turning yellow),

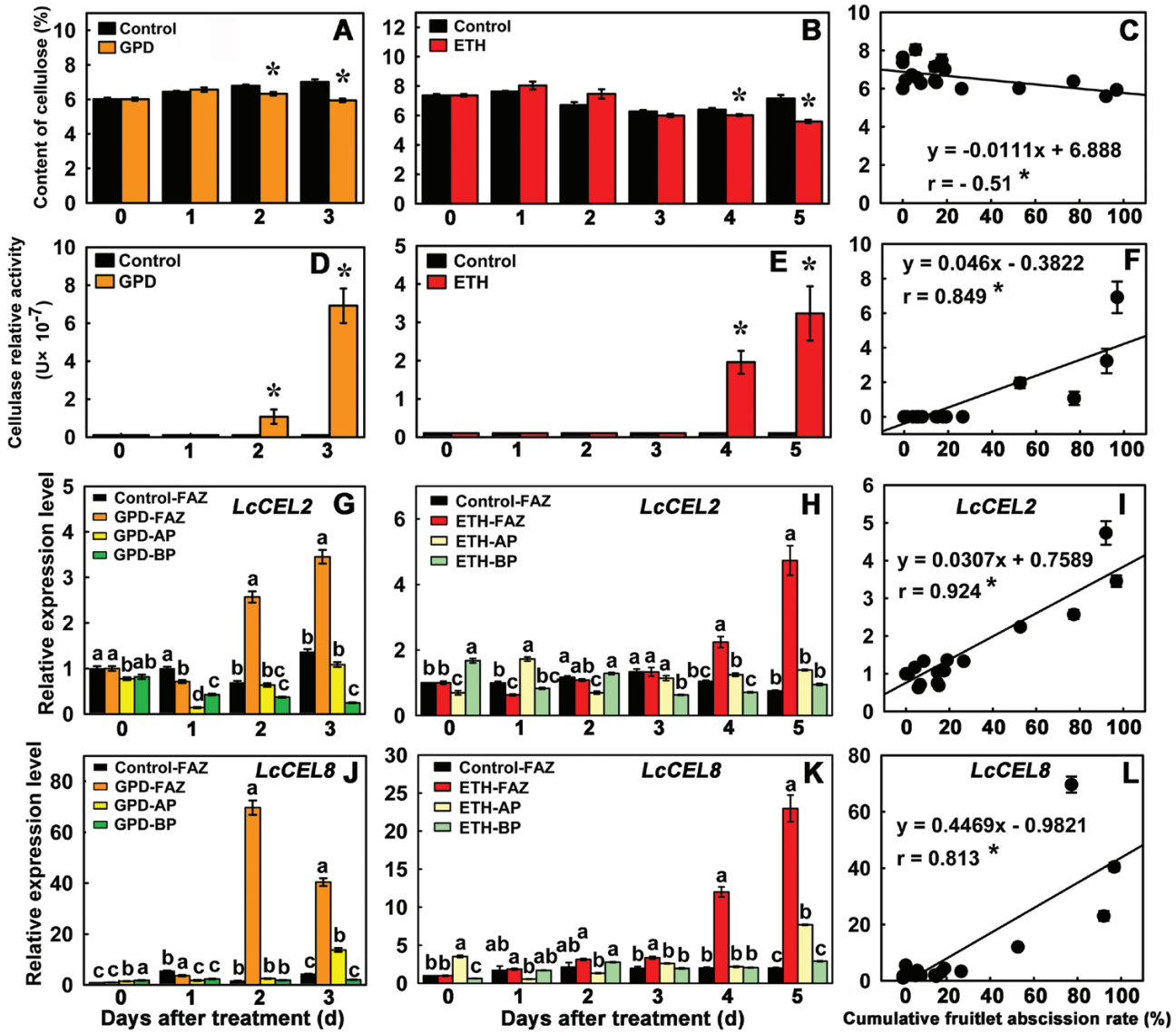

Fig. 3. Effects of two abscission-accelerating treatments on cellulose content (A-C), cellulase activity (D-F), and gene expression of *LcCEL2* (G–I) and *LcCEL8* (J–L) during fruitlet abscission in litchi. (A, D, G, J) Samples collected after girdling plus defoliation (GPD). (B, E, H, K) Samples collected after treatment with ethephon (ETH). (C, F, I, L) Correlations between the cumulative fruitlet abscission rate and (C) cellulose content, (F) cellulase activity, and expression of (I) *LcCEL2* and (L) *LcCEL8* in the fruitlet abscission zone. Data are means (±SE) from three replicates. Significant differences between treated and control branches in (A, B, D, E) were determined using Student's *t*-test: $^{**}P<0.01$. Different letters in (G, H, J, K) indicate significant differences as determined using Duncan's multiple range test ($P<0.05$). The correlation coefficients (r) are significant at $^{*}P<0.05$ (C, F, I, L). FAZ, fruitlet abscission zone; AP, apical portion of pedicel; BP, basal portion of pedicel (see Methods and Supplementary Fig. S1B).

encompassing the replum, the valve margins, and the funiculi (Fig. 5A, C, D). GUS signals in *proCEL8::GUS* plants were exclusively in the abscission regions, such as the flower AZs from position 3 onward, the dehiscence and seed-shedding zones of the siliques, and the base of cauline leaves (Fig. 5B, E–G). Collectively, these data demonstrated that *LcCEL2* and *LcCEL8* probably have important functions during the abscission of plant organs.

LcHB2 activates the expression of LcCEL2 *and* LcCEL8 *by directly binding to their promoters*

To characterize potential regulators of *LcCEL2* and *LcCEL8*, their promoter sequences were further analysed for core *cis*-elements and other motifs. We found that the promoters of both genes contained two HD-binding *cis*-elements (Supplementary Dataset S1). The *LcCEL2* promoter had two HD-binding *cis*-elements: AAATTAAA at position −95 to −46 relative to the start of transcription, and AAATTAGT at position −725 to −676 relative to the start of transcription. Interestingly, the *LcCEL8* gene promoter contained binding sites for HD-Zip TFs at position −1589 to −1540 (TAAATGCA) relative to the transcription start site and at position −2076 to −2027 (AAATTAGT) relative to the transcription start site. The promoter regions of both *LcCEL2* and *LcCEL8* contained the AAATTAGT binding motif. We hypothesized that *LcCEL2* and *LcCEL8* might be directly regulated by HD-Zip TFs in litchi. In our previous RNA-Seq analyses, we identified an HD-ZIP unigene (L10059562) with significantly increased expression after ethylene induction of fruitlet abscission (Li

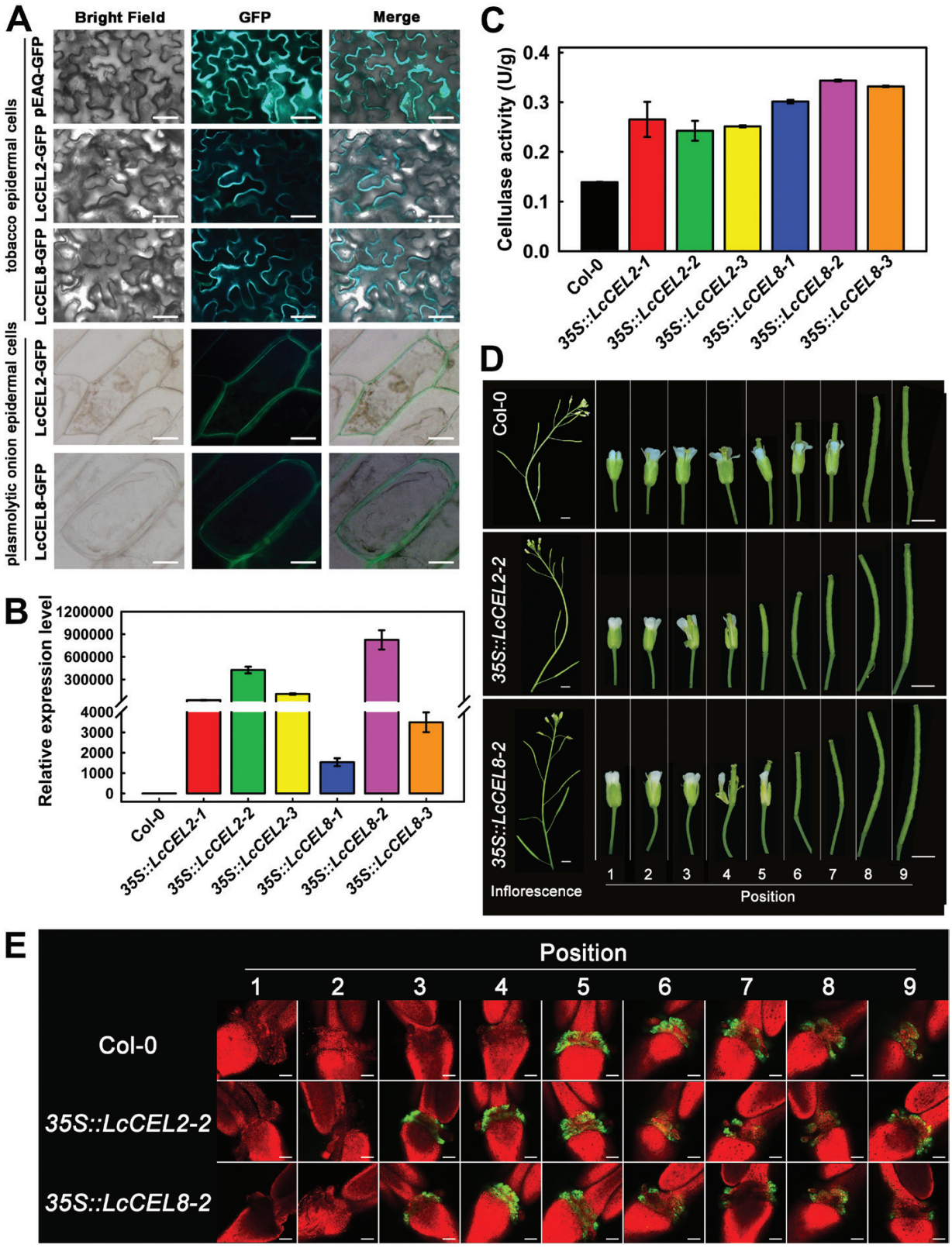

Fig. 4. Functional analysis of litchi *LcCEL2* and *LcCEL8*. (A) Subcellular localization of LcCEL2-GFP and LcCEL8-GFP fusion proteins in tobacco leaves and plasmolytic onion epidermal cells. (B) Expression of *LcCEL2* and *LcCEL8* in leaves of different transgenic Arabidopsis plants. The *35S::LcCEL2-1*, *35S::LcCEL2-2*, and *35S::LcCEL2-3* lines ectopically expressed *LcCEL2* under the control of the CaMV 35S promoter in wild-type plants (Col-0). The *35S::LcCEL8-1*, *35S::LcCEL8-2*, and *35S::LcCEL8-3* lines ectopically expressed *LcCEL8* under the control of the CaMV 35S promoter in Col-0. *AtUBQ* was used as an internal control for qRT-PCR analysis. The *y*-axis represents the fold-change in the expression levels relative to Col-0. Data are means (±SE) from three replicates. (C) Cellulase activity in leaves of different transgenic Arabidopsis plants. Data are means (±SE) from three replicates. (D) Phenotypes of floral organ abscission in transgenic Arabidopsis lines. Position numbers were counted from the first flower with visible white petals at the top of the inflorescence. (E) BCECF fluorescence micrographs of floral organ abscission zones in transgenic Arabidopsis lines. The images represent BCECF fluorescence merged with chlorophyll autofluorescence. An increase in pH is indicated by green fluorescence; chlorophyll autofluorescence is in red. Representative images are shown from 3–4 replicates in total. Scale bars are 25 μm (A), 3 mm (D), and 100 μm (E).

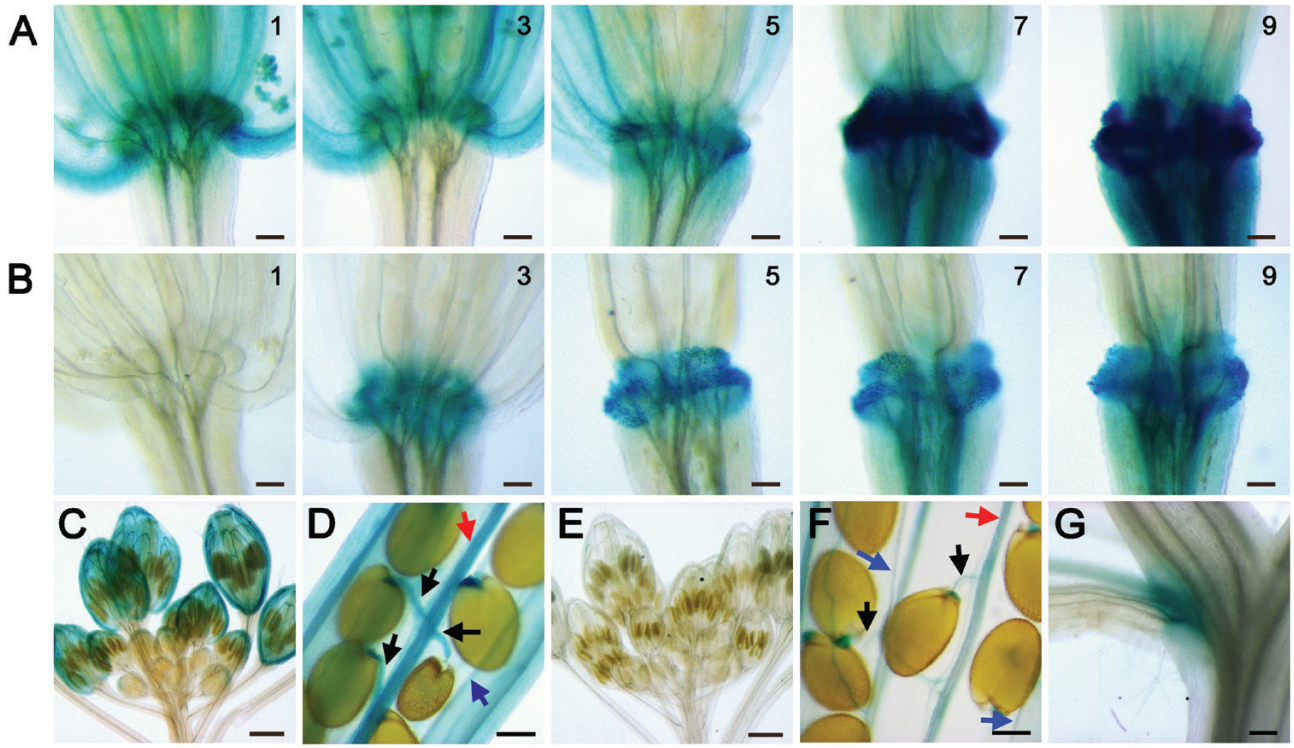

Fig. 5. GUS expression driven by the litchi *LcCEL2* and *LcCEL8* promoters in transgenic Arabidopsis. (A) GUS expression in the abscission zone at positions 1, 3, 5, 7, and 9 along the inflorescence for *proLcCEL2::GUS*. (B) GUS expression in the abscission zone at positions 1, 3, 5, 7, and 9 along the inflorescence for *proLcCEL8::GUS*. Position numbers were counted from the first flower with visible white petals at the top of the inflorescence. (C, D) GUS expression in (C) floral buds and (D) siliques (turning yellow) for *proLcCEL2::GUS*. (E–G) GUS expression in (E) floral buds, (F) silique (turning yellow), and (G) cauline leaves for *proLcCEL8::GUS*. Arrows indicate funiculi (black), replums (red), and valve margins (blue). Scale bars are 100 μm (A, B, D, F), 300 μm (G), and 500 μm (C, E).

et al., 2015b). In the present study, we cloned the full-length cDNA and designated this gene as *LcHB2*. Phylogenetic analysis showed that LcHB2 clustered with ATHB7, ATHB12, and CsHB18 in the HD-Zip I subfamily (Supplementary Fig. S6). *LcHB2* was expressed exclusively and strongly in the FAZs, with expression highest at day 1 after GPD (~8.5-fold) (Fig. 6A) and at day 4 after ETH treatment (~44-fold) (Fig. 6B). The expression of *LcHB2* in the FAZs was significantly positively correlated with the cumulative fruitlet abscission rate (Fig. 6C). *In vivo* subcellular localization analysis revealed that the LcHB2 protein was located in the nucleus (Fig. 6D). Furthermore, dual-luciferase assays showed that the LcHB2 protein acted as a transcriptional activator *in vivo* (Fig. 6E). These results demonstrated that LcHB2 was a genuine TF that could activate the expression of downstream genes. In addition, *LcHB2* promoter activity was examined using a promoter::GUS transgene (*proLcHB2::GUS*). The GUS signals were strongly detected in the abscission regions, such as the flower AZs from position 5 onward, the dehiscence zones of the siliques (replum and valve margins), the seed-shedding zone (funiculi), and the base of cauline leaves (Fig. 6F–H). The GUS signal also appeared in anther filaments and petals (Fig. 6F).

To examine the function of LcHB2 in the regulation of expression of *LcCEL2* and *LcCEL8*, we performed transient expression assays using a dual-luciferase system. Compared with the empty-vector control, the ratio of LUC/REN expression was significantly increased when the pEAQ-LcHB2 effector construct was co-transfected with either the *proLcCEL2*-LUC or the *proLcCEL8*-LUC reporter construct (Fig. 7A, B), confirming that LcHB2 is a transcriptional activator of *LcCEL2* and *LcCEL8*. EMSAs were performed to test whether LcHB2 could bind to the HD-binding *cis*-elements in the *LcCEL2* and *LcCEL8* promoters. Four DNA fragments (~50 bp) containing HD-binding *cis*-elements in the promoter regions of *LcCEL2* and *LcCEL8* were synthesized and labeled with biotin. The recombinant histidine-tagged (His)-LcHB2 fusion protein was expressed in *E. coli* BL21 (DE3) cells and purified (Fig. 7C). We found that recombinant LcHB2 protein could bind strongly to the *LcCEL2* and *LcCEL8* promoter fragments, and that this binding could be abolished by high amounts of competitive unlabeled sequences that were otherwise identical, but not by promoter sequences containing mutant binding sites (Fig. 7D, E). Mobility shifts were not observed if the *LcCEL2* and *LcCEL8* promoter fragments were incubated with poly-His alone (Fig. 7D, E). Thus, *LcCEL2* and *LcCEL8* are direct targets of LcHB2, which activates the expression of these two genes by directly binding to their promoters.

Discussion

The fruitlet abscission zone (FAZ) in litchi where fruitlets detach from maternal plants is located at the pedicel–fruitlet junction (Supplementary Fig. S1B) and consists of 7–10 layers of small cells with dense cytoplasm that are histologically distinct from their surrounding cells (Fig. 1). We explored the changes

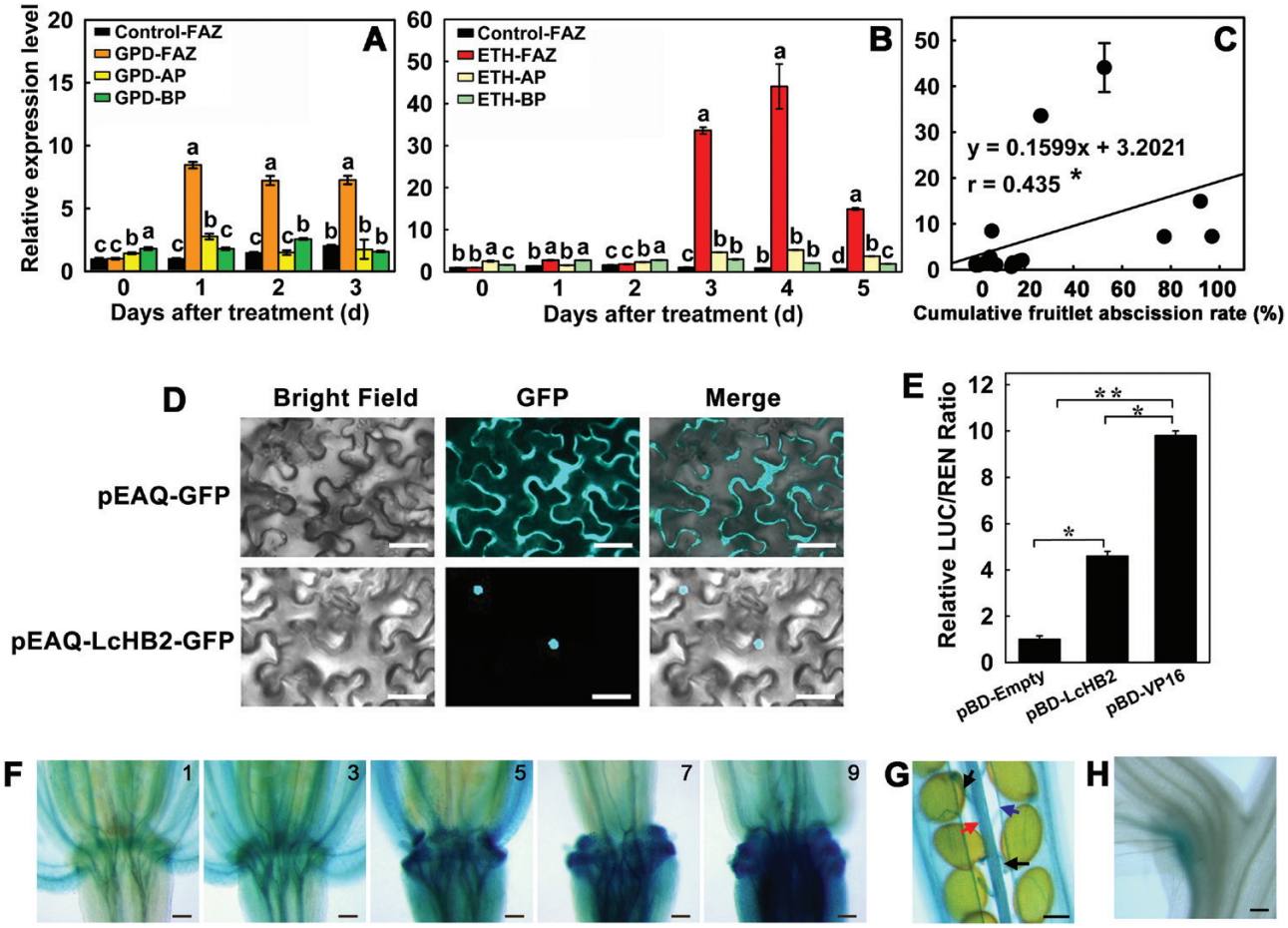

Fig. 6. Expression patterns, subcellular localization, and the transcriptional activation function of LcHB2 protein in litchi. (A, B) Effects of girdling plus defoliation (GPD) and treatment with ethephon (ETH) on the expression of *LcHB2* in the fruitlet abscission zones (FAZs) and two pedicel regions flanking the FAZs, the apical portion (AP) at the fruitlet side above the FAZ and the basal portion (BP) below the FAZ. (C) Correlation between the cumulative fruitlet abscission rate and the expression level of *LcHB2* in the FAZ. Data in (A–C) are means (±SE) from three replicates. Different letters indicate significant differences as determined using Duncan's multiple range test ($P<0.05$). The correlation coefficient (r) is significant at $^{*}P<0.05$. (D) Nuclear localization of LcHB2-GFP in tobacco leaves. Scale bars are 25 μm. (E) Transcriptional activation function of LcHB2 in tobacco leaves, as indicated by the ratio of LUC to REN expression. Data are means (±SE) from six replicates. Significant differences between means were determined using Student's *t*-test: $^{*}P<0.05$, $^{**}P<0.01$. (F–H) GUS expression driven by the *LcHB2* promoter in transgenic Arabidopsis. (F) GUS expression in the abscission zone at positions 1, 3, 5, 7, and 9 along the inflorescence for *proLcHB2::GUS*. Position numbers were counted from the first flower with visible white petals at the top of the inflorescence. (G, H) GUS expression in (G) the siliques (turning yellow) and (H) cauline leaves for *proLcHB2::GUS*. Arrows indicate funiculi (black), replums (red), and valve margins (blue). Scale bars are 100 μm (F, G), and 300 μm (H).

in the microscopic structure of FAZs during fruitlet abscission under two abscission-accelerating treatments, namely carbohydrate deficiency (caused by girdling plus defoliation, GPD) and application of ethephon (ETH). GPD completely blocks the carbohydrate transport to fruits and leads to a serious carbohydrate stress for fruit development (Obeso, 1998; Gómez-Cadenas *et al.*, 2000), while ethylene is known to accelerate abscission of plant organs (Taylor and Whitelaw, 2001). Cell separation in FAZs was clearly observed following these two treatments in our study. The disruption of cells initiated in the stem cortex and epidermis and spread toward the vascular bundle and pith regions in the FAZ. Significant increases in the sizes of FAZ cells were also observed (Fig. 1; Supplementary Fig. S3). Similar enlargement in abscission zone cells has previously been observed in flower AZs of soybean (*Glycine max*; Oberholster *et al.*, 1991) and tomato (Tabuchi *et al.*, 2001), in floral AZs of Arabidopsis (Shi *et al.*, 2011), in leaf AZs of olive (*Olea europaea*; Kitsaki *et al.*, 1999), and in fruit AZs of apple (Pandita and Jindal, 1991) and citrus (cv. 'Shamouti', Huberman *et al.*, 1988; cv. 'Satsuma Mandarin' and 'Kiyomi', Li *et al.*, 2017). Enlargement of separation zone cells is the result of tension across intact walls that is released during separation (Sexton and Roberts, 1982), and it may be the earliest conspicuous structural change that is characteristic of organ shedding. The enlargement of cells may generate the tension needed for final rupture of the FAZ in litchi.

During swelling and expansion, FAZ cells lose their anisotropic properties, suggesting that great changes are taking place in the cell wall architecture. High cellulase activity appears to be characteristic of developmental processes during which cell wall architecture is disrupted, including organ abscission (Sexton *et al.*, 1980; Brummell *et al.*, 1999) and pod dehiscence (Chauvaux *et al.*, 1997). Thus, it was not surprising to find cellulase activity associated with litchi fruitlet abscission (Figs 3, 4), because increased activity seems to be a feature of separating AZs (Sexton *et al.*, 1980; Trainotti et al., 1998a, 1998b;

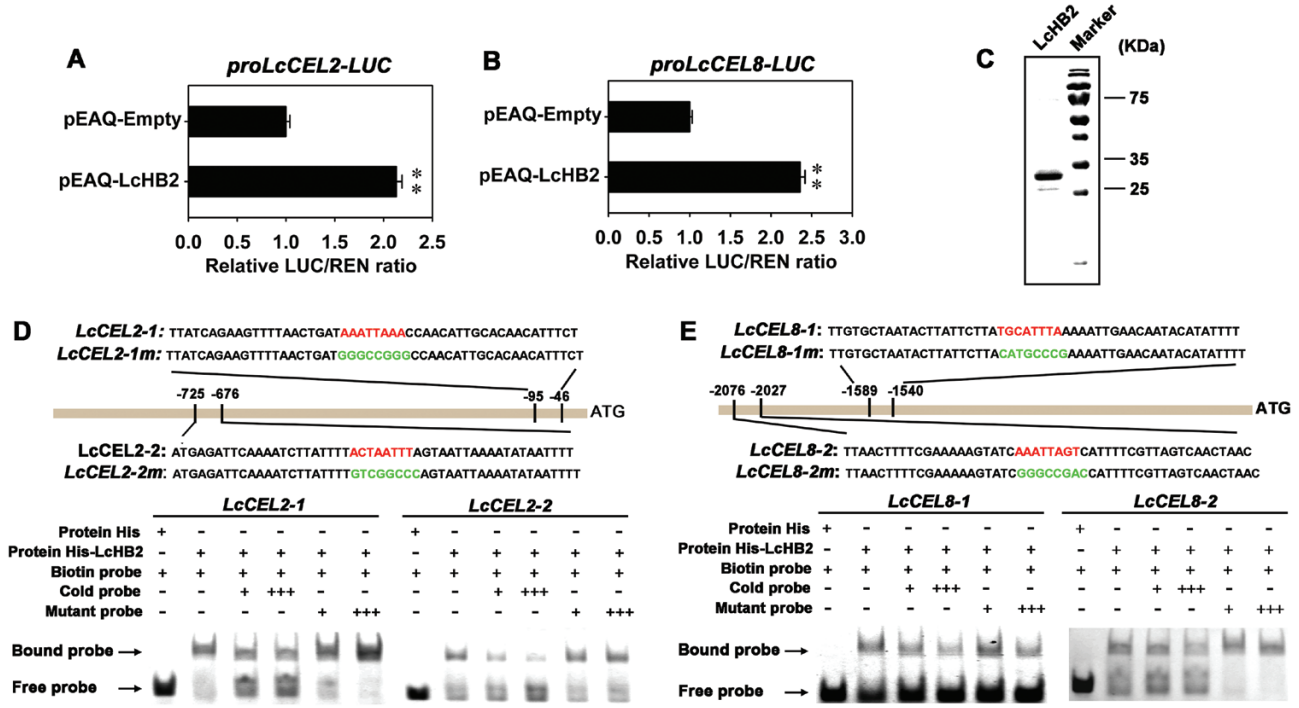

Fig. 7. Binding of LcHB2 to *LcCEL2* and *LcCEL8* promoters and activation of their activities. LcHB2 activates the expression of *LcCEL2* (A) and *LcCEL8* (B) *in vivo* as indicated by transient dual-luciferase reporter assays in tobacco leaves. The ratio of LUC/REN expression of the empty vector (pEAQ) plus promoter was used as a calibrator (set to 1). Data are means (±SE) from six replicates. Significant differences between means were determined using Student's *t*-test: ** $P<0.01$. (C) SDS-PAGE gel stained with Coomassie Brilliant Blue demonstrating affinity purification of the recombinant LcHB2 protein. (D, E) Electrophoretic mobility shift assays (EMSAs) showing the association of LcHB2 with the *LcCEL2* and *LcCEL8* promoters *in vitro*. Sequences of both the wild-type and mutant probes are shown at the top. The core HD-binding *cis*-elements are indicated in red and the mutant elements are indicated in green. Shifted bands, suggesting the formation of DNA–protein complexes, are indicated by arrows. '–' and '+' represent an absence or presence, respectively. '+++' indicates increasing amounts of unlabeled or mutated probes introduced for competition. A non-biotin-labeled probe was added as an unlabeled competitor.

Brummell *et al.*, 1999). We have assumed that the natural substrate for the cellulase that we measured is cellulose, the predominant insoluble cell wall polysaccharide that is composed of D-glucose moieties joined by β(1→4) linkages into a linear molecule (O'Brien *et al.*, 1964). In our present study, the strong loss in intensity of PAS, Calcofluor White, and CBM3a staining in walls of abscising FAZ cells that we observed after GPD or ETH treatment suggested that the polysaccharide constituents, or to be more exact, cellulose, decreased exclusively at the onset of cell separation (Fig. 2). We also found increases in cellulase activities and corresponding decreases in cellulose contents in abscising FAZs (Fig. 3A, B), confirming that cellulases are involved in degrading cellulose during cell separation of in the abscission zone of litchi fruitlets.

The accumulation of a cellulase-encoding mRNA induced by ethylene treatment was first reported in abscising bean leaves (Tucker *et al.*, 1988). Since then, several studies have demonstrated that cellulase activity and gene expression are correlated with events in AZs during shedding of plant organs (in avocado, Tonutti *et al.*, 1995; in tomato, del Campillo and Bennett, 1996; in pepper, *Capsicum annuum*, Trainotti *et al.*, 1997; and in citrus, Kazokas and Burns, 1998). Cellulases are encoded by a multigene family, as confirmed in our study that identified 20 cellulase genes in the litchi genome. Among these, the abscission-specific expression of *LcCEL2* and *LcCEL8* were followed by enhanced cellulase activities and subsequently by decreased cellulose contents in FAZ cells (Fig. 3). Although many abscission-related cellulase genes have also been identified in the FAZ tissues of several other fruit crop species (Trainotti *et al.*, 1997; Li *et al.*, 2010; Merelo *et al.*, 2017), our understanding of the functions of these cellulases during fruit abscission is limited. Here, overexpression of *LcCEL2* and *LcCEL8* in Arabidopsis was able to accelerate floral organ abscission, and analysis of GUS-promoter fusion lines further showed that these genes were expressed in cells in the AZ during floral organ abscission and silique dehiscence (Figs 4D, E, 5; Supplementary Fig. S5), suggesting that *LcCEL2* and *LcCEL8* are functionally involved in abscission.

Interestingly, the LcCEL2 and LcCEL8 proteins were not highly conserved with each other and showed only 49% similarity. Compared to cellulases in other plants (Supplementary Fig. S7), LcCEL8 had higher similarity to abscission-related cellulases in citrus (CitCEL6; Merelo *et al.*, 2017), peach (PpEG1; Trainotti *et al.*, 1997), tomato (SlCel5; Kalaitzis *et al.*, 1999), and pepper (cCel2; Trainotti *et al.*, 1998b), while LcCEL2 was more closely related to cotton (*Gossypium hirsutum*) GhCel1 (Mishra *et al.*, 2008) and peach PpEG4 (Trainotti *et al.*, 2006). These data might not seem surprising if the comparisons refer only to the structure of the polypeptides rather than to their functions *in vivo*. Still, proteins from the subfamilies to which LcCEL2 and LcCEL8 belong seem more likely to be involved in organ abscission than do members of other cellulase families. Notably,

the *LcCEL2* and *LcCEL8* promoters could drive *GUS* expression not only in the floral AZ but also in the dehiscence zones of the siliques in Arabidopsis, encompassing the replum, the valve margins, and the funiculi. (Fig. 5), indicating that *LcCEL2* and *LcCEL8* might also affect silique dehiscence in transgenic Arabidopsis. In addition, the GUS signal in *proLcCEL2::GUS* plants was present in the stigmatic tissues, anther filaments, and petals, suggesting that *LcCEL2* might also affect floral organ development.

HD-Zip TFs are a large class of plant TFs that are widely involved in the regulation of different growth and developmental processes. Although no study has directly confirmed whether HD-Zip TFs control plant organ shedding, high-throughput gene expression analyses have shown that HD-Zip genes encode differentially expressed TFs that might have central roles in the shedding of organs (e.g. in tomato flowers, Meir *et al.*, 2010; apple fruitlets, Zhu *et al.*, 2011; Heo *et al.*, 2016; olive fruit, Gil-Amado and Gomez-Jimenez, 2013; soybean leaves, Kim *et al.*, 2016; and rose petals, Gao *et al.*, 2016). Indeed, transcripts of a putative HD-Zip gene (*LcHB2*) did show significantly increased abundance during the abscission of litchi fruitlets upon carbohydrate stress or application of ethylene (Fig. 6). LcHB2 belongs to one of the four subfamilies (I–IV) of HD-Zip TFs, which show binding preferences for variant HD-binding motifs (Sessa et al., 1993, 1998; Palena *et al.*, 2001; Lin *et al.*, 2008; Tominaga-Wada *et al.*, 2009; Xu *et al.*, 2014). The Arabidopsis cellulase gene At2g32990 contains three such HD-binding motifs in its promoter that allow its transcription to be directly regulated by an HD-Zip IV TF (HDG11) to promote root elongation and enhance drought tolerance (Xu *et al.*, 2014). It is noteworthy that At2g32990 has also been reported to be involved in cell wall remodeling in Arabidopsis stamen AZs (Lashbrook and Cai, 2008).

In our study, *LcCEL2* and *LcCEL8* associated with fruitlet abscission in litchi also contained two HD-binding *cis*-elements in their promoters. Further experiments confirmed that LcHB2 could directly bind with promoter segments from *LcCEL2* and *LcCEL8* that contained an HD-binding *cis*-element and hence serve as a transcriptional activator for these genes (Fig. 7). Notably, accumulation of *LcHB2* transcripts occurred earlier than *LcCEL2* and *LcCEL8* transcripts, which further supports the hypothesized role of LcHB2 as an upstream regulator of these two cellulase genes. HD-Zip TFs participate in responses to environmental cues including abiotic stress and stresses mediated by ABA (Johannesson *et al.*, 2003; Olsson *et al.*, 2004; Ariel *et al.*, 2007, 2010; Romani *et al.*, 2016), in leaf or floral development (Kim *et al.*, 2007; Lin *et al.*, 2008), root elongation (Miao *et al.*, 2018), flower senescence (Chang *et al.*, 2014; Lü *et al.*, 2014), and fruit ripening (Lin *et al.*, 2008; Jiang *et al.*, 2017). Here, we demonstrated that an HD-Zip TF is also involved in organ shedding through regulation of the expression of cellulase genes. Interestingly, the regulation of abscission- or dehiscence-related cellulase genes by HD-Zip TFs is probably conserved among plant species, as at least one HD-binding *cis*-element was found in the promoter regions of 17 cellulase-encoding genes from six plant species (Supplementary Fig. S8, Supplementary Dataset S1).

Taken our results together, we propose that LcHB2 may act as a positive regulator of fruitlet abscission through directly activating *LcCEL2* and *LcCEL8* in litchi. When fruitlets sense abscission signals such as carbohydrate deficiency or ethylene stimuli, the expression levels of *LcHB2* are up-regulated. *LcCEL2* and *LcCEL8* expressed specifically i the FAZ are induced by LcHB2 via direct binding to their promoters, and cellulase activities are increased. Cellulose contents are therefore reduced, and ultimately fruitlets abscise due to cell wall degradation and cell separation in the FAZ.

Supplementary data

Supplementary data are available at *JXB* online.

Fig. S1. Illustration of girdling and the pedicel samples examined in this study.

Fig. S2. Constructs used in this study.

Fig. S3. Effects of ethephon treatment on cumulative fruitlet abscission rate, phenotypic performance, and cell separation in the FAZ.

Fig. S4. Expression profiles of 20 cellulase genes from litchi after GPD and ETH treatments.

Fig. S5. Overexpression of *LcCEL2* and *LcCEL8* causes earlier floral organ abscission in Arabidopsis.

Fig. S6. Multiple sequence alignments and phylogenetic analysis of LcHB2 with other plant HD-Zip proteins.

Fig. S7. Multiple sequence alignments and phylogenetic analysis of LcCEL2 and LcCEL8.

Fig. S8. Diagram of 17 promoters of abscission-related cellulase genes from various plant species.

Table S1. List of primers used in this study.

Table S2. Characteristics of cellulase and HD-Zip proteins from litchi.

Table S3. Presence of cellulase genes identified in this study in other plant species.

Table S4. Presence of HD-Zip genes identified in this study in other plant species.

Table S5. RPKM values of 20 cellulase genes of litchi identified in the transcriptomes of plants in the GPD and ETH treatments.

Dataset S1. Nucleotide sequences of the promoters of *LcHB2* and 19 cellulase genes.

Acknowledgements

This work was supported by funds from the Natural Science Foundation of China (Grant Nos 31772269, 31600152, and 31070159), the Postdoctoral Science Foundation of China (Grant No. 2015M572329), the Innovation Team Project of the Department of Education of Guangdong Province (2016KCXTD011), the Guangzhou Science and Technology Key Project (201804020063), and the Outstanding Talent Program of the Ministry of Agriculture, and the China Agricultural Research System (CARS-33-11). We would like to thank Dr Chunlin Shi (Department of Biosciences, University of Oslo) for critically reading and assisting with drafting this manuscript, and Mary Ann Cushman (Alum Canyon Editing, LLC) for her helpful and critical English language editing.

Author contributions

CL, JL, HW, and MZ designed the study; CL, XM, ZW, PY, and MP performed the experiments; MZ and XN provided critical technical assistance; CL and JL wrote the manuscript with contributions from all the authors; CL, JL, MZ, HW, and RX supervised the project, interpreted the data, and revised the manuscript. All authors read and approved the final manuscript.

References

Ariel F, Diet A, Verdenaud M, Gruber V, Frugier F, Chan R, Crespi M. 2010. Environmental regulation of lateral root emergence in *Medicago truncatula* requires the HD-Zip I transcription factor HB1. The Plant Cell **22**, 2171–2183.

Ariel FD, Manavella PA, Dezar CA, Chan RL. 2007. The true story of the HD-Zip family. Trends in Plant Science **12**, 419–426.

Blake AW, McCartney L, Flint JE, Bolam DN, Boraston AB, Gilbert HJ, Knox JP. 2006. Understanding the biological rationale for the diversity of cellulose-directed carbohydrate-binding modules in prokaryotic enzymes. The Journal of Biological Chemistry **281**, 29321–29329.

Bourgault R, Bewley JD. 2002. Gel diffusion assays for endo-beta-mannanase and pectin methylesterase can underestimate enzyme activity due to proteolytic degradation: a remedy. Analytical Biochemistry **300**, 87–93.

Brummell DA, Hall BD, Bennett AB. 1999. Antisense suppression of tomato endo-1,4-beta-glucanase Cel2 mRNA accumulation increases the force required to break fruit abscission zones but does not affect fruit softening. Plant Molecular Biology **40**, 615–622.

Chang X, Donnelly L, Sun D, Rao J, Reid MS, Jiang CZ. 2014. A Petunia homeodomain-leucine zipper protein, PhHD-Zip, plays an important role in flower senescence. PLoS ONE **9**, e88320.

Chauvaux N, Child R, John K, Ulvskov P, Borkhardt B, Prinsen E, Van Onckelen HA. 1997. The role of auxin and cell separation in the dehiscence zone of oilseed rape pods. Journal of Experimental Botany **48**, 1423–1429.

Clough SJ, Bent AF. 1998. Floral dip, a simplified method for *Agrobacterium*-mediated transformation of *Arabidopsis thaliana*. The Plant Journal **16**, 735–743.

del Campillo E, Bennett AB. 1996. Pedicel breakstrength and cellulase gene expression during tomato flower abscission. Plant Physiology **111**, 813–820.

Estornell LH, Agusti J, Merelo P, Talon M, Tadeo FR. 2013. Elucidating mechanisms underlying organ abscission. Plant Science **199**, 48–60.

Feder NED, O'Brien TP. 1968. Plant microtechnique, some principles and new methods. American Journal of Botany **55**, 123–142.

Gao Y, Liu C, Li X, Xu H, Liang Y, Ma N, Fei Z, Gao J, Jiang CZ, Ma C. 2016. Transcriptome profiling of petal abscission zone and functional analysis of an Aux/IAA family gene *RhIAA16* involved in petal shedding in rose. Frontiers in Plant Science **7**, 1375.

Gilamado JA, Gomez-Jimenez MC. 2013. Transcriptome analysis of mature fruit abscission control in olive. Plant & Cell Physiology **54**, 244–269.

Gómez-Cadenas A, Mehouachi J, Tadeo FR, Primo-Millo E, Talon M. 2000. Hormonal regulation of fruitlet abscission induced by carbohydrate shortage in citrus. Planta **210**, 636–643.

He H, Bai M, Tong P, Hu Y, Yang M, Wu H. 2018. CELLULASE6 and MANNANASE7 affect cell differentiation and silique dehiscence. Plant Physiology **176**, 2186–2201.

Heo S, Hwang JH, Jun JH, Lee HJ. 2016. Abscission-related genes revealed by RNA-Seq analysis using self-abscising apple (*Malus×domestica*). Journal of Pomology & Horticultural Science **91**, 271–278.

Hieke S, Menzel CM, Doogan VJ, Ludders P. 2002. The relationship between yield and assimilate supply in lychee (*Litchi chinensis* Sonn.). Journal of Horticultural Science & Biotechnology **77**, 326–332.

Horton RF, Osborne DJ. 1967. Senescence, abscission and cellulase activity in *Phaseolus vulgaris*. Nature **214**, 1086–1088.

Huberman ME, Zamski E, Goren R. 1988. Anatomical changes induced by ethylene in the abscission zone of citrus leaf and fruit explants. Israel Journal of Plant Sciences **37**, 107–121.

Hughes J, McCully ME. 1975. The use of an optical brightener in the study of plant structure. Stain Technology **50**, 319–329.

Jiang Y, Liu C, Yan D, *et al*. 2017. *MdHB1* down-regulation activates anthocyanin biosynthesis in the white-fleshed apple cultivar 'Granny Smith'. Journal of Experimental Botany **68**, 1055–1069.

Johannesson H, Wang Y, Hanson J, Engström P. 2003. The *Arabidopsis thaliana* homeobox gene *ATweHB5* is a potential regulator of abscisic acid responsiveness in developing seedlings. Plant Molecular Biology **51**, 719–729.

Kalaitzis P, Hong SB, Solomos T, Tucker ML. 1999. Molecular characterization of a tomato endo-beta-1,4-glucanase gene expressed in mature pistils, abscission zones and fruit. Plant & Cell Physiology **40**, 905–908.

Kazokas WC, Burns JK. 1998. Cellulase activity and gene expression in citrus fruit abscission zones during and after ethylene treatment. Journal of the American Society for Horticultural Science **123**, 781–786.

Kim J, Yang J, Yang R, Sicher RC, Chang C, Tucker ML. 2016. Transcriptome analysis of soybean leaf abscission identifies transcriptional regulators of organ polarity and cell fate. Frontiers in Plant Science **7**, 125.

Kim YK, Son O, Kim MR, Nam KH, Kim GT, Lee MS, Choi SY, Cheon CI. 2007. *ATHB23*, an Arabidopsis class I homeodomain-leucine zipper gene, is expressed in the adaxial region of young leaves. Plant Cell Reports **26**, 1179–1185.

Kitsaki CK, Drossopoulos JB, Aivalakis G, Anastasiadou F, Delis C. 1999. *In vitro* studies of ABA and ethephon induced abscission in olive organs. Journal of Pomology & Horticultural Science **74**, 19–25.

Koehler SM, Matters GL, Nath P, Kemmerer EC, Tucker ML. 1996. The gene promoter for a bean abscission cellulase is ethylene-induced in transgenic tomato and shows high sequence conservation with a soybean abscission cellulase. Plant Molecular Biology **31**, 595–606.

Kuang JF, Wu JY, Zhong HY, Li CQ, Chen JY, Lu WJ, Li JG. 2012. Carbohydrate stress affecting fruitlet abscission and expression of genes related to auxin signal transduction pathway in litchi. International Journal of Molecular Sciences **13**, 16084–16103.

Lashbrook CC, Cai S. 2008. Cell wall remodeling in *Arabidopsis* stamen abscission zones: temporal aspects of control inferred from transcriptional profiling. Plant Signaling & Behavior **3**, 733–736.

Lashbrook CC, Giovannoni JJ, Hall BD, Fischer RL, Bennett AB. 1998. Transgenic analysis of tomato endo-β-1,4-glucanase gene function role of *cel1* in floral abscission. The Plant Journal **13**, 303–310.

Lashbrook CC, Gonzalez-Bosch C, Bennett AB. 1994. Two divergent endo-beta-1,4-glucanase genes exhibit overlapping expression in ripening fruit and abscising flowers. The Plant Cell **6**, 1485–1493.

Li C, Wang Y, Huang X, Li J, Wang H, Li J. 2015a. An improved fruit transcriptome and the identification of the candidate genes involved in fruit abscission induced by carbohydrate stress in litchi. Frontiers in Plant Science **6**, 439.

Li C, Wang Y, Ying P, Ma W, Li J. 2015b. Genome-wide digital transcript analysis of putative fruitlet abscission related genes regulated by ethephon in litchi. Frontiers in Plant Science **6**, 502.

Li JG, Yuan RC. 2008. NAA and ethylene regulate expression of genes related to ethylene biosynthesis, perception, and cell wall degradation during fruit abscission and ripening in 'Delicious' apples. Journal of Plant Growth Regulation **27**, 283–295.

Li JG, Zhu H, Yuan RC. 2010. Profiling the expression of genes related to ethylene biosynthesis, ethylene perception, and cell wall degradation during fruit abscission and fruit ripening in apple. Journal of the American Society for Horticultural Science **135**, 391–401.

Li X, Kitajima A, Kataoka K, Takisawa R, Nakazaki T. 2017. Anatomical observations of the citrus fruit abscission zone and morphological changes of the cells during secondary physiological fruit drop. Journal of the Japanese Society for Horticulture Science **86**, 447–455.

Lin Z, Hong Y, Yin M, Li C, Zhang K, Grierson D. 2008. A tomato HD-Zip homeobox protein, LeHB-1, plays an important role in floral organogenesis and ripening. The Plant Journal **55**, 301–310.

Lü P, Zhang C, Liu J, Liu X, Jiang G, Jiang X, Khan MA, Wang L, Hong B, Gao J. 2014. RhHB1 mediates the antagonism of gibberellins to

ABA and ethylene during rose (*Rosa hybrida*) petal senescence. The Plant Journal **78**, 578–590.

Meir S, Philosoph-Hadas S, Sundaresan S, Selvaraj KS, Burd S, Ophir R, Kochanek B, Reid MS, Jiang CZ, Lers A. 2010. Microarray analysis of the abscission-related transcriptome in the tomato flower abscission zone in response to auxin depletion. Plant Physiology **154**, 1929–1956.

Merelo P, Agustí J, Arbona V, *et al*. 2017. Cell wall remodeling in abscission zone cells during ethylene-promoted fruit abscission in citrus. Frontiers in Plant Science **8**, 301.

Miao ZQ, Zhao PX, Mao JL, Yu LH, Yuan Y, Tang H, Liu ZB, Xiang CB. 2018. HOMEOBOX PROTEIN52 mediates the crosstalk between ethylene and auxin signaling during primary root elongation by modulating auxin transport-related gene expression. The Plant Cell **30**, 2761–2778.

Mishra A, Khare S, Trivedi PK, Nath P. 2008. Effect of ethylene, 1-MCP, ABA and IAA on break strength, cellulase and polygalacturonase activities during cotton leaf abscission. South African Journal of Botany **74**, 282–287.

Mitra SK, Pereira LS, Pathak PK, Majumdar D. 2003. Fruit abscission pattern of lychee cultivars. Acta Horticulturae **665**, 215–218.

Nicholas KB. 1997. GeneDoc, analysis and visualization of genetic variation. EMBNEW. NEWS **4**, 14.

O'Brien TP, Feder N, McCully ME. 1964. Polychromatic staining of plant cell walls by toluidine blue O. Protoplasma **59**, 368–373.

Oberholster SD, Peterson CM, Dute RR. 1991. Pedicel abscission of soybean, cytological and ultrastructural changes. Canadian Journal of Botany **69**, 2177–2186.

Obeso JR. 1998. Effects of defoliation and girdling on fruit production in *Ilex aquifolium*. Functional Ecology **12**, 486–491.

Olsson AS, Engström P, Söderman E. 2004. The homeobox genes *ATHB12* and *ATHB7* encode potential regulators of growth in response to water deficit in *Arabidopsis*. Plant Molecular Biology **55**, 663–677.

Palena CM, Tron AE, Bertoncini CW, Gonzalez DH, Chan RL. 2001. Positively charged residues at the N-terminal arm of the homeodomain are required for efficient DNA binding by homeodomain-leucine zipper proteins. Journal of Molecular Biology **308**, 39–47.

Pandita VK, Jindal KK. 1991. Enzymatic and anatomical changes in abscission zone cells of apple fruits induced by ethephon. Biologia Plantarum **33**, 20–25.

Patterson SE. 2001. Cutting loose. abscission and dehiscence in *Arabidopsis*. Plant Physiology **126**, 494–500.

Puchooa D. 2004. A simple, rapid and efficient method for the extraction of genomic DNA from lychee (*Litchi chinensis* Sonn.). African Journal of Biotechnology **3**, 253–255.

Qi WE, Chen HB, Li WW, Zhang HJ. 2016. Development situation, trend and suggestions of Chinese litchi industry. Guangdong Agricultural Sciences **43**, 173–179.

Reid PD, Lewis LN. 1974. Cellulase and abscission in the red kidney bean (*Phaseolus vulgaris*). Plant Physiology **53**, 732–737.

Roberts JA, Elliott KA, Gonzalez-Carranza ZH. 2002. Abscission, dehiscence, and other cell separation processes. Annual Review of Plant Biology **53**, 131–158.

Romani F, Ribone PA, Capella M, Miguel VN, Chan RL. 2016. A matter of quantity: common features in the drought response of transgenic plants overexpressing HD-Zip I transcription factors. Plant Science **251**, 139–154.

Sessa G, Morelli G, Ruberti I. 1993. The ATHB-1 and -2 HD-ZIP domains homodimerize forming complexes of different DNA binding specificities. The EMBO Journal **12**, 3507–3517.

Sessa G, Steindler C, Morelli G, Ruberti I. 1998. The *Arabidopsis ATHB-8*, *-9* and *-14* genes are members of a small gene family coding for highly related HD-ZIP proteins. Plant Molecular Biology **38**, 609–622.

Sexton R, Durbin ML, Lewis LN, Thomson WW. 1980. Use of cellulase antibodies to study leaf abscission. Nature **283**, 873–874.

Sexton R, Roberts JA. 1982. Cell biology of abscission. Annual Review of Plant Biology **33**, 133–162.

Shi CL, Stenvik GE, Vie AK, Bones AM, Pautot V, Proveniers M, Aalen RB, Butenko MA. 2011. Arabidopsis class I KNOTTED-like homeobox proteins act downstream in the IDA-HAE/HSL2 floral abscission signaling pathway. The Plant Cell **23**, 2553–2567.

Stern RA, Kigel J, Tomer E, Gazit S. 1995. 'Mauritius' lychee fruit development and reduced abscission after treatment with the auxin 2,4,5-TP. Journal of the American Society for Horticultural Science **120**, 65–70.

Sundaresan S, Philosoph-Hadas S, Riov J, Belausov E, Kochanek B, Tucker ML, Meir S. 2014. Abscission of flowers and floral organs is closely associated with alkalization of the cytosol in abscission zone cells. Journal of Experimental Botany **66**, 913–919.

Tabuchi T, Ito S, Arai N. 2001. Anatomical studies of the abscission process in the tomato pedicels at flowering stage. Journal of the Japanese Society for Horticultural Science **70**, 63–65.

Tamura K, Peterson D, Peterson N, Stecher G, Nei M, Kumar S. 2011. MEGA5: molecular evolutionary genetics analysis using maximum likelihood, evolutionary distance, and maximum parsimony methods. Molecular Biology and Evolution **28**, 2731–2739.

Taylor JE, Whitelaw CA. 2001. Signals in abscission. New Phytologist **151**, 323–340.

Thompson DS, Higgins DG, Gibson TJ. 1994. CLUSTAL W: improving the sensitivity of progressive multiple sequence alignment through sequence weighting, position-specific gap penalties and weight matrix choice. Nucleic Acids Research **22**, 4673–4680.

Tominaga-Wada R, Iwata M, Sugiyama J, Kotake T, Ishida T, Yokoyama R, Nishitani K, Okada K, Wada T. 2009. The GLABRA2 homeodomain protein directly regulates *CESA5* and *XTH17* gene expression in Arabidopsis roots. The Plant Journal **60**, 564–574.

Tonutti P, Cass LG, Christoffersen RE. 1995. The expression of cellulase gene family members during induced avocado fruit abscission and ripening. Plant, Cell & Environment **18**, 709–713.

Trainotti L, Ferrarese L, Casadoro G. 1998a. Characterization of cCel3, a member of the pepper endo-beta-1,4-glucanase multigene family. Hereditas **128**, 121–126.

Trainotti L, Ferrarese L, Poznanski E, Vecchia FD. 1998b. Endo-β-1,4-glucanase activity is involved in the abscission of pepper flowers. Journal of Plant Physiology **152**, 70–77.

Trainotti L, Pavanello A, Zanin D. 2006. *PpEG4* is a peach endo-beta-1,4-glucanase gene whose expression in climacteric peaches does not follow a climacteric pattern. Journal of Experimental Botany **57**, 589–598.

Trainotti L, Spolaore S, Ferrarese L, Casadoro G. 1997. Characterization of *ppEG1*, a member of a multigene family which encodes endo-beta-1,4-glucanase in peach. Plant Molecular Biology **34**, 791–802.

Tucker ML, Baird SL, Sexton R. 1991. Bean leaf abscission: tissue-specific accumulation of a cellulase mRNA. Planta **186**, 52–57.

Tucker ML, Sexton R, Del Campillo E, Lewis LN. 1988. Bean abscission cellulase: characterization of a cDNA clone and regulation of gene expression by ethylene and auxin. Plant Physiology **88**, 1257–1262.

Tucker ML, Whitelaw CA, Lyssenko NN, Nath P. 2002. Functional analysis of regulatory elements in the gene promoter for an abscission-specific cellulase from bean and isolation, expression, and binding affinity of three TGA-type basic leucine zipper transcription factors. Plant Physiology **130**, 1487–1496.

Urbanowicz BR, Bennett AB, Del Campillo E, *et al*. 2007. Structural organization and a standardized nomenclature for plant endo-1,4-beta-glucanases (cellulases) of glycosyl hydrolase family 9. Plant Physiology **144**, 1693–1696.

Viles FJ Jr, Silverman L. 1949. Determination of starch and cellulose with anthrone. Analytical Chemistry **21**, 950–953.

Wang L, Liu GS, Wang LS, Zhang ZH, Hou JH, Guo HM. 1998. The optimal conditions for cellulase activity measurement with DNS method. Journal of Henan Normal University **26**, 66–69.

Wang X, Liu D, Li A, Sun X, Zhang R, Wu L, Liang Y, Mao L. 2013. Transcriptome analysis of tomato flower pedicel tissues reveals abscission zone-specific modulation of key meristem activity genes. PLoS ONE **8**, e55238.

Xu P, Cai XT, Wang Y, Xing L, Chen Q, Xiang CB. 2014. HDG11 upregulates cell-wall-loosening protein genes to promote root elongation in Arabidopsis. Journal of Experimental Botany **65**, 4285–4295.

Yang Z, Zhong X, Fan Y, Wang H, Li J, Huang X. 2015. Burst of reactive oxygen species in pedicel-mediated fruit abscission after carbohydrate supply was cut off in longan (*Dimocarpus longan*). Frontiers in Plant Science **6**, 360.

Ye YJ, Xiao YY, Han YC, Shan W, Fan ZQ, Xu QG, Kuang JF, Lu WJ, Lakshmanan P, Chen JY. 2016. Banana fruit VQ motif-containing protein5 represses cold-responsive transcription factor MaWRKY26 involved in the regulation of JA biosynthetic genes. Scientific Reports **6**, 23632.

Ying P, Li C, Liu X, Xia R, Zhao M, Li J. 2016. Identification and molecular characterization of an IDA-like gene from litchi, *LcIDL1*, whose ectopic expression promotes floral organ abscission in *Arabidopsis*. Scientific Reports **6**, 37135.

Yuan RC, Huang HB. 1988. Litchi fruit abscission, its patterns, effect of shading and relation to endogenous abscisic acid. Scientia Horticulturae **36**, 281–292.

Zhong HY, Chen JW, Li CQ, Chen L, Wu JY, Chen JY, Lu WJ, Li JG. 2011. Selection of reliable reference genes for expression studies by reverse transcription quantitative real-time PCR in litchi under different experimental conditions. Plant Cell Reports **30**, 641–653.

Zhu H, Dardick CD, Beers EP, Callanhan AM, Xia R, Yuan R. 2011. Transcriptomics of shading-induced and NAA-induced abscission in apple (*Malus domestica*) reveals a shared pathway involving reduced photosynthesis, alterations in carbohydrate transport and signaling and hormone crosstalk. BMC Plant Biology **11**, 138.

Zou LP, Sun XH, Zhang ZG, Liu P, Wu JX, Tian CJ, Qiu JL, Lu TG. 2011. Leaf rolling controlled by the homeodomain leucine zipper class IV gene *Roc5* in rice. Plant Physiology **156**, 1589–1602.